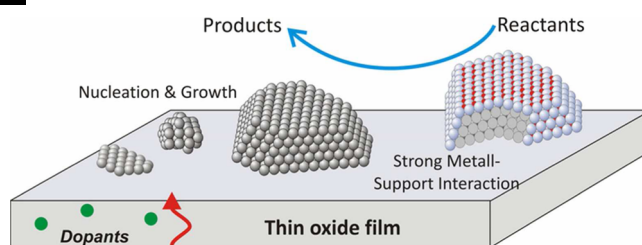# Nanoparticles for Heterogeneous Catalysis: New Mechanistic Insights

SWETLANA SCHAUERMANN, NIKLAS NILIUS,
SHAMIL SHAIKHUTDINOV, AND HANS-JOACHIM FREUND*

Department of Chemical Physics, Fritz-Haber-Institut der Max-Planck-Gesellschaft, Faradayweg 4-6, 14195 Berlin, Germany

RECEIVED ON AUGUST 6, 2012

CONSPECTUS

Metallic nanoparticles finely dispersed over oxide supports have found use as heterogeneous catalysts in many industries including chemical manufacturing, energy-related applications and environmental remediation. The compositional and structural complexity of such nanosized systems offers many degrees of freedom for tuning their catalytic properties. However, fully rational design of heterogeneous catalysts based on an atomic-level understanding of surface processes remains an unattained goal in catalysis research.

Researchers have used surface science methods and metal single crystals to explore elementary processes in heterogeneous catalysis. In this Account, we use more realistic materials that capture part of the complexity inherent to industrial catalysts. We assess the impacts on the overall catalytic performance of characteristics such as finite particle size, particle structure, particle chemical composition, flexibility of atoms in clusters, and metal−support interactions.

To prepare these materials, we grew thin oxide films on metal single crystals under ultrahigh vacuum conditions and used these films as supports for metallic nanoparticles. We present four case studies on specifically designed materials with properties that expand our atomic-level understanding of surface chemistry. Specifically, we address (1) the effect of dopants in the oxide support on the growth of metal nanoclusters; (2) the effects of size and structural flexibility of metal clusters on the binding energy of gas-phase adsorbates and their catalytic activity; (3) the role of surface modifiers, such as carbon, on catalytic activity and selectivity; and (4) the structural and compositional changes of the active surface as a result of strong metal−support interaction. Using these examples, we demonstrate how studies of complex nanostructured materials can help revealing atomic processes at the solid−gas interface of heterogeneous catalysts. Among our findings is that doping of oxide materials opens promising routes to alter the morphology and electronic properties of supported metal particles and to induce the direct dissociation and reaction of molecules bound to the oxide surface. Also, the small size and atomic flexibility of metal clusters can have an important influence on gas adsorption and catalytic performance.

Introduction

Heterogeneously catalyzed processes constitute the basis for a large number of chemical technologies employed nowadays. The range of applications of heterogeneous catalysis covers chemical manufacturing, energy harvesting, conversion and storage, to environmental technology.[1] Many commercially important catalysts comprise catalytically active nanoparticles dispersed on high area oxide supports. Such catalysts are typically highly complex multicomponent materials that are optimized to work for millions of turnovers, at high reaction rates, and with high selectivity. Often, additives are introduced to promote their activity, selectivity, and stability.[1] The compositional and structural complexity of these catalysts allows tuning the chemical and adsorption properties in order to optimize their performance in a specific reaction. This enormous

complexity of real catalysts renders an atomistic understanding of the structure−reactivity relationships challenging. As a consequence, real supported catalysts may be modeled by simpler systems, which are chosen to capture a certain degree of complexity. The employment of well-defined model systems consisting of metal−particle ensembles supported on planar oxide substrates, thus stepping beyond models of clean single crystal metal surfaces, has proven to provide a successful approach to achieve fundamental insights into the catalysis on nanostructured surfaces.[2−4] In the last two decades, a number of fundamental aspects governing catalytic activity, such as the influence of finite article size and the oxide−metal interface, were addressed by employing this model catalysts approach. Most of these studies were performed on atomically clean surfaces and under ultrahigh vacuum conditions. In this Account, we will go beyond these studies by adding additional structural complexity inherent to realistic catalysts or realistic catalytic processes. Particularly, we will address following fundamental questions: How can particle size and shape be controlled by doping impurity ions of different valence into the oxide support? How does the binding energy of reactants depend on the particle size? What is the role of surface modifiers such as, for example, carbonaceous deposits, which are usually formed on transitions metals under operation conditions, in catalytic conversions of hydrocarbons? What is the role of the strong metal−support interaction and what consequences does this have for the catalytic performance under realistic reaction conditions? With these case studies, we will illustrate some of the key aspects of heterogeneous catalysis based on metal nanoparticles.

Controlling the Shape of Supported Metal Nanoparticles via Doping the Oxide Support

The performance of metal particles in catalytic reactions is governed by their size and shape as well as by interactions with the oxide support.[5−9] A good fraction of the catalysis research was therefore devoted to tailor the shape of metal deposits on oxide surfaces. One parameter that controls the particle geometry is the metal−support interaction, which is typically small for wide-gap oxides, causing the admetals to grow in a 3D fashion.[3] Several approaches were developed to modify this parameter, for instance, via introducing defects and adspecies (hydroxyl groups) into the oxide surface or using polar oxide terminations with high metal−oxide adhesion. Alternatively, electron-transfer processes across the metal−oxide interface may be exploited to alter the
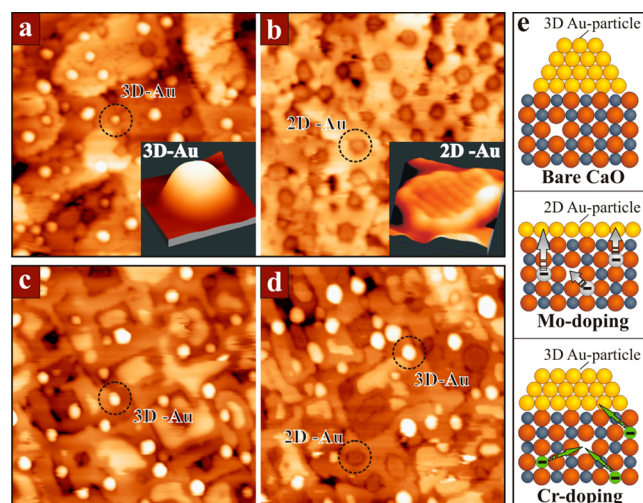

FIGURE 1. STM images of (a) bare and (b) Mo-doped CaO(001) films of 60 ML thickness after dosing 0.5 ML of Au (60 × 50 nm², +6.0 V). 2D Au islands appear as depressions on the insulting oxide, because electron transport into the gold is inhibited at the high scanning bias. Insets show typical 3D and 2D islands taken at lower bias (3.5 V, 10 × 10 nm²). Similar measurements on (c) bare and (d) Cr-doped MgO(001) films of 20 ML thickness. Particle shape is not affected by the dopants in this case. (e) Ball models explaining the charge transfer from the doped oxide to the admetal and their influence on the particle shape.

growth morphology of metals. This approach has been demonstrated for thin-film oxides on metal supports first.[10] There, electron tunnelling through the insulting film leads to spontaneous charging of the particles and activates new coupling schemes to the oxide support, for example, Coulomb or polaronic interactions. Examples for the charge-driven stabilization of unusual particle shapes are the 1D Au chains formed on alumina[11] and the 2D Au islands on MgO[12] and CaO films.[13]

However, the concept of geometry control via charge transfer is not limited to ultrathin films, but can be extended to bulk oxides as used in catalysis. One obvious approach is the insertion of dopants into the oxide volume, which act as intrinsic charge donors/acceptors depending on their valence state with respect to the original ions.[14,15] For example, high-valence dopants are able to transfer extra electrons into the admetal, which in turn modify the equilibrium geometry as discussed before. The impact of donor-type impurities on the growth morphology of metals could be shown for CaO doped with 1−2% Mo.[16] While only the common 3D growth regime is observed for Au deposition onto pure CaO(001), formation of monolayer Au islands is revealed for the doped films (Figure 1b). The change in growth morphology reflects the donor character of the Mo dopants that initially adopt a 2+ charge state. In the presence of Au adatoms, electrons are transferred from the
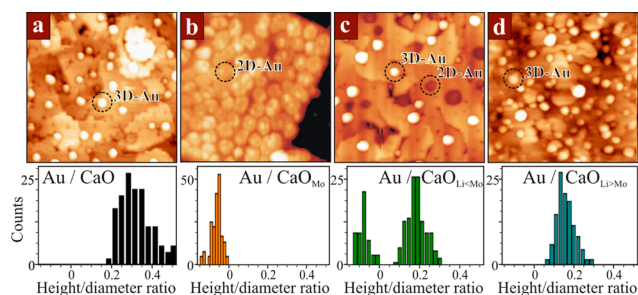
FIGURE 2. STM images of 0.5 ML Au deposited onto (a) pristine CaO, (b) doped with 4% Mo, (c) doped with 4% Mo + 2% Li, and (d) doped with 4% Mo + 8% Li (50×50 nm^2, 6.0 V). Note that monolayer Au islands in (b) and (c) appear as depressions at high sample bias. Histogram of the particle shapes (height-to-diameter) are plotted below. Note the transitions from 2D to 3D particles when balancing the high-valence Mo dopants with monovalent Li impurities.

energetically unfavorable Mo 4d crystal field levels into Au-induced acceptor states, being much lower in energy.[16] As a result, the Mo ions get oxidized while Au turns anionic and becomes subject to reinforced bonding to the CaO surface (Figure 1e). The so generated Mo^{3+} species may act as charge donors as well, as the highest occupied crystal-field state still lies above the Au 6s affinity level, and even Mo^{4+} is able to transfer electrons toward gold.[17] It is this multivalent nature of Mo that is responsible for the robust donor characteristic of CaO$_{Mo}$.

Interestingly, Cr dopants in a MgO lattice hardly modify the Au growth regime and most deposits retain their initial 3D geometry (Figure 1c,d).[17] The weak donor character of Cr is explained with a substantial stabilization of the Cr d-electrons in the MgO crystal field, giving rise to low-lying Cr t_{2g}-levels in the band gap. As a result, each Cr dopant donates only a single excess electron, which may not even reach the gold due to parasitic electron traps present in the MgO films, for example, line defects and cationic vacancies (Figure 1e).[18] The weak donor strength of Cr in conjunction with competing charge traps in the host oxide explains why, in contrast to CaO$_{Mo}$, MgO$_{Cr}$ does not alter the growth morphology of gold.

The impact of high-valence dopants on the shape of metal particles can, to a certain extent, be reversed by low-valence dopants (Figure 2). Cations with lower charge state than the host ions generate holes in the oxide electronic structure that are able to trap the excess electrons provided by the donors. We have shown such a compensation effect for CaO films codoped with Li and Mo ions.[19] As long as the Mo dopant level exceeds the one of Li, 2D Au islands form on the surface because charge transfer into the gold remains active (Figure 2b,c). However, more and more Au deposits

turn 3D as the Li concentration rises, because the Mo excess electrons get captured by Li-induced holes states and do not reach the admetal anymore (Figure 2d). We note that the very same charge-transfer processes that modify the shape of metal adparticles will be active for molecular adsorption as well and might, for example, lead to the spontaneous dissociation or activation of O$_2$ on doped oxide surfaces.

Binding Energy of Adsorbates: Particle Size Effects

The performance of a heterogeneous catalyst strongly depends on the bond strength of the adsorbed surface species and on the relative thermodynamic stabilities of the reaction intermediates. It is one of the most important fundamental questions in catalysis research: How does the strength of a molecule−particle bond depend on the size of supported metal nanoparticle?

We addressed this question by the direct calorimetric measurement of adsorption enthalpies of gas phase molecules on well-defined Pd nanoparticles supported on a Fe$_3$O$_4$(111)/Pt(111) film.[20] The energetics of interaction of carbon monoxide with well-defined metal nanoparticles were previously studied indirectly by desorption-based methods,[2,21] which did not provide a clear trend in the changes of the adsorption energy with particles size. Application of single crystal adsorption calorimetry allows to overcome the restrictions imposed by the kinetic modeling of desorption processes[22,23] and to directly measure the binding energy of adsorbates as a function of particle size.

To address the dependence of the CO adsorption energy on particle size, five different supported model systems with nominal Pd deposition thicknesses of 0.3, 0.6, 1.5, 4, and 7 Å (Figure 3) were investigated. These Pd coverages correspond to particles containing between 120 and 4900 Pd atoms per particle or sizes between 1.8 and 8 nm diameter. The dependence of initial CO adsorption heats (corresponding to adsorption of a few CO molecules per Pd nanoparticle) on particle size shows a pronounced trend: the initial heat of adsorption decreases with decreasing particle size, from 126 $\pm$ 7 kJ·mol^{-1} on 8 nm Pd particles to 106 $\pm$ 2 kJ·mol^{-1} on 1.8 nm clusters. Additionally, all investigated particles showed smaller initial adsorption enthalpy as compared to the single crystal surface (149 kJ·mol^{-1}).

The surfaces of the Pd particles investigated in this work expose mainly (111) terraces alongside with a smaller fraction of (100) facets and low-coordinated sites such as edges and corners. According to theoretical calculations[24] and experimental evidence (see discussion in ref 17), such
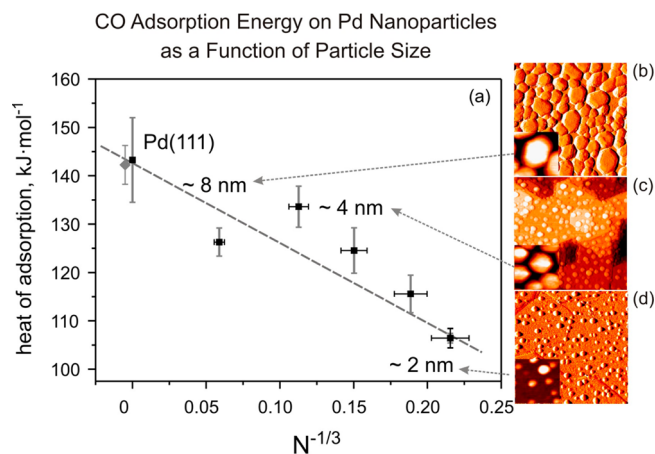
FIGURE 3. (a) Initial heat of adsorption of CO as a function of Pd particle size.[20] The gray symbol corresponds to the literature value on Pd(111). (b–d) STM images of the Pd/Fe$_3$O$_4$/Pt(111) model catalyst (100 × 100 nm, inset 20 × 20 nm) for nominal Pd coverage of (b) 0.3 Å, (c) 4 Å, and (d) 7 Å.[20]

irregular sites exhibit only slightly higher CO adsorption energies than Pd(111). This suggests that the degree of coordination of the surface atoms on stepped surfaces is not as important in determining CO adsorption energies on Pd as on other metals like Pt.[25] Therefore, the increasing fraction of low-coordination Pd atoms with decreasing particle size, which normally would be expected to lead to higher adsorption energies for CO, might not be the dominant effect in determining how CO adsorption energies vary with particle size for Pd. Instead, other size-dependent properties of a Pd nanocluster must be responsible for the observed decrease of the initial adsorption enthalpy of carbon monoxide with decreasing the particle size.

Two alternative microscopic effects may contribute to the observed decrease of the initial CO adsorption heat with decreasing particle size: (i) weakening of the chemisorptive interaction and (ii) reduction of the van der Waals attraction. First, the decrease of the chemisorption energy can result from the contraction of the lattice parameter of a small metal nanoparticle, which was demonstrated experimentally[26] and predicted theoretically.[27] This phenomenon has been rationalized to result from the decreasing average coordination number of atoms with higher surface-to-volume ratio of the cluster.[27] This lattice contraction in small metal clusters was theoretically shown to result in a reduction of the adsorbate binding energy.[28] Particularly for CO adsorption on the Pd clusters consisting of 55–260 atoms, it was demonstrated that clusters with optimized structures show systematically lower adsorption energies by about 10–15 kJ·mol^{-1} than clusters with a bulk terminated geometry, i.e.

with all interatomic distances d(Pd–Pd) = 275 pm. This finding agrees with the principle of bond order conservation:[29] in "contracted" clusters, one expects weaker adsorption bonds and stronger binding within the adsorbate as a result of saturated valences among the substrate atoms. Such effects were found not to be restricted to 3-fold hollow sites on (111) facets, but reflect a general trend that also holds for adsorption at other sites of particles such as bridge sites and edges. Note that for the even smaller clusters in the subnanometer size range, theoretical calculations predict (on average) increasing adsorption energy with decreasing cluster size mainly due to quantum effects that become essential for such small aggregates.[30] The experimental verification of this prediction for the subnanometer sized clusters was not possible in this study due to experimental reasons.

A second reason for heats of adsorption of a gas-phase molecule on the small metal clusters to decrease is a feasible weakening of dispersion force (van der Waals interaction) that is induced by the dynamic response of bulk electrons of the metal to charge density fluctuations in an adsorbed molecule. The large overall magnitude of the decrease in the heat of adsorption, obtained in our study (about 40 kJ·mol^{-1} relative to the Pd(111) surface), allows us to suggest that most likely reduction of both van der Waals interaction and chemisorption strength contributes to the overall decrease of the adsorption heat.

Recently, the binding strength of atomic oxygen at the edges of large Pd nanoclusters was experimentally shown to be higher than on Pd(111), in clear contrast to situation found for CO. In addition, decreasing particles size was found to result in a strong decrease of oxygen binding energy at the particle edges, similarly to the trend discussed above for CO.[31] This finding suggests a general nature of the observed particle size dependence for a broad range of adsorbates.

Kinetics of Surface Reactions: Effects of Surface Modifiers and Atomic Flexibility of Metallic Nanoparticles

Real catalytic processes often require small amounts of some additives (promoters), such as, for example, alkali metals or halogens,[1] that ensure high catalytic activity and selectivity. The role that these compounds play at a microscopic level remains unclear for most of the known catalytic systems in operation. One of the most important coadsorbates, particularly in hydrocarbon chemistry, is carbon resulting from decomposition of the reactants. Accumulation of carbon was recognized to considerably affect the activity and the selectivity in hydrocarbon conversions promoted by
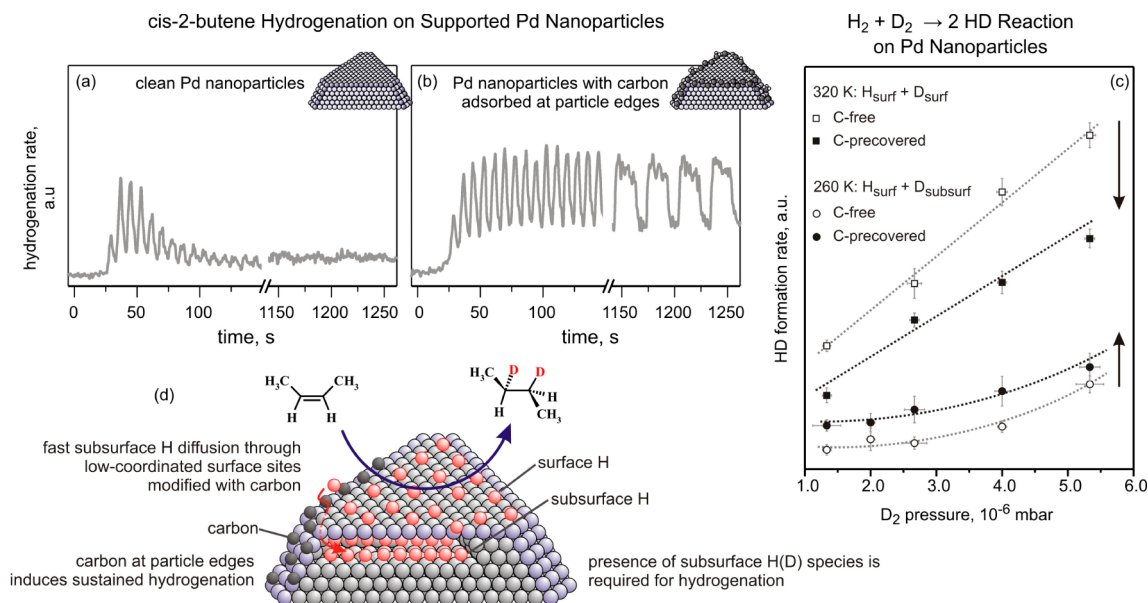
FIGURE 4. Hydrogenation rate of *cis*-2-butene at 260 K over clean (a) and C-precovered (b) model catalysts Pd/Fe$_3$O$_4$/Pt(111).[33] (c) Steady state HD formation rates obtained on the pristine and C-precovered Pd nanoparticles supported on Fe$_3$O$_4$/Pt(111) at 260 and 320 K. (d) Proposed reaction mechanism of olefin hydrogenation on Pd nanoparticles. Pancels (c) and (d) adapted with permission from ref 40. Copyright 2012 American Chemical Society.

transition metals.[32] In our studies, by comparing the hydrogenation activity of clean and C-containing Pd nanoparticles we addressed the underlying microscopic mechanisms of C-induced changes in the catalytic performance for hydrogenation of olefins.[33−35]

Hydrogenation rates of *cis*-2-butene over clean and C-containing Pd nanoparticles supported on Fe$_3$O$_4$(111)/Pt(111) film are shown in Figure 4a. Pd nanoparticles were saturated first with deuterium to form both surface and subsurface D species[36] and then short pulses of *cis*-2-butene were applied. Clean Pd nanoparticles exhibit high hydrogenation activity for an initial short period of time (a few butene pulses), after which it drops to zero. In contrast, if carbon was deposited on Pd nanoparticles prior the reaction, a sustained hydrogenation rate was observed. Using CO as a probe molecule for different adsorption sites, it can be shown that deposited carbon modifies the low-coordinated site such as edges and corners.[33] However, it is not clear whether carbon resides on the surface or might penetrate into the subsurface region as predicted theoretically.[37] This effect demonstrates the exceptional importance of carbon for olefin hydrogenation, which can be carried out in a truly catalytic fashion for many turnovers, only on C-containing Pd nanoparticles.

The role of carbon in promotion of sustained hydrogenation was rationalized by employing transient molecular beam experiments and resonant nuclear reaction analysis

(rNRA) for hydrogen depth profiling. First, we obtained the first direct experimental evidence that the presence of H(D) absorbed in the Pd particle volume is required for olefin hydrogenation, particularly for the second half-hydrogenation step,[33] in agreement with previous experimental evidence.[38] This result explains the high initial hydrogenation rates, observed on the clean particles fully saturated with D, and vanishing hydrogenation activity in steady state because of the depletion of the subsurface D reservoir (Figure 4a). Apparently, the inability to populate subsurface D sites arises from hindered D subsurface diffusion through the surface covered with hydrocarbons. Further, it was shown that even a submonolayer coverage of carbon significantly affects the H(D) depth distribution in Pd particles.[33] Based on these observations, and on the analysis of the hydrogenation kinetics,[35] we attribute the sustained hydrogenation activity to facilitation of H(D) diffusion into the particle volume by deposited carbon.

The proposed mechanism was confirmed both theoretically[39] and experimentally.[40] Computational studies on Pd nanoclusters demonstrated that deposited carbon dramatically enhances the hydrogen diffusion rate into subsurface, mainly due to a local elongation of Pd−Pd bonds and a concomitant lowering of the activation barrier.[39] This dramatic reduction of the activation barrier can account for the experimentally observed unusual promotion of sustained hydrogenation activity by carbon. In contrast, the lateral

rigidity of the extended Pd(111) surface was predicted to hinder this effect, in agreement with experimental observations.[34] The results demonstrate the conceptual importance of atomic flexibility of sites near particle edges, which, in contrast to intrinsically rigid regular single crystal surfaces, play a crucial role in H subsurface diffusion on Pd.

Finally, we provided direct experimental evidence for a faster subsurface H diffusion through C-modified low-coordinated surface sites on Pd nanoparticles by probing the diffusion rate via $H_2 + D_2 \rightarrow HD$ exchange in different temperature regimes.[40] It was previously shown[36] that the formation of HD can occur either via recombination of two surface H and D species or an involvement of subsurface H or D species. The latter pathway dominates at low temperatures between 200 and 300 K. Our experimental results are consistent with the scenario implying that one subsurface atom (H or D) recombines with a surface-adsorbed atom to form HD. In the case of slow subsurface H(D) diffusion, the formation rate of subsurface species will be the limiting step in HD production, and can, therefore, be addressed by probing the rate of isotopic scrambling.

Figure 4c shows the steady state HD formation rates at 260 and 320 K on clean and C-modified Pd nanoparticles. Carbon modification of the particles edges was found to affect the HD formation rate in a dramatically different way for two reaction temperatures: whereas at 320 K preadsorbed C *reduces* the overall reaction rate by about 30%, the reaction rate *increases* by about 100% at 260 K on the C-modified particles. The decreased HD formation rate at 320 K, where HD formation is dominated by the recombination of the surface H and D species,[36] can be rationalized as a consequence of the blocking of surface adsorption sites by carbon. Interestingly, even though a part of the surface is blocked by carbon, the HD formation rate is significantly increased at 260 K, where desorption involves at least one subsurface H(D) species. This effect can be explained only by the higher formation rate of the subsurface H(D) species on the C-modified particles, resulting in a higher steady state concentration of subsurface species.

Such insight allowed us to identify an exceptionally important role of carbon in hydrogenation chemistry on nanostructured catalysts that was previously not clearly appreciated. According to our model, small amounts of carbon modify the low-coordinated surface site of Pd nanoclusters (edges, corners), thus allowing for effective replenishment of subsurface H in steady state and enabling with this sustained hydrogenation. These results also highlight the crucial role of subsurface H diffusion, which is a strongly structure-sensitive process on Pd surfaces, in hydrogenation of the olefinic bond. Computational studies suggest that the atomic flexibility of the low-coordinated surface sites is an important structural feature that is responsible for easy subsurface diffusion of H under operation condition.

Modeling Strong Metal/Support Interaction

The term "Strong Metal−Support Interaction (SMSI)" has been originally used to describe the decreased chemisorption capacity for CO and H_2 on metal particles supported on reducible oxides after heat treatment, most notably observed for Pt supported on TiO_2.[41] One explanation put forward is the encapsulation of the metal by the support oxide. The atomic structure of the encapsulated layer is often unknown.[42,43] It is intuitively expected that the encapsulation will inhibit reactions by suppressing adsorption of molecules otherwise readily adsorbing on a metal surface. It has, however, recently been shown[44] that the surface modification of a metal particle by an overgrown oxide film may even lead to enhanced catalytic activity if the chemical potential of the gas phase is set properly. Here, we address this issue using model systems consisting of (i) Pt nanoparticles supported on Fe_3O_4(111) and (ii) thin iron oxide films on Pt(111).

Figure 5a shows Pt nanoparticles deposited at 300 K and annealed in UHV at 850 K. Owing to the good epitaxial relationships between Fe_3O_4(111) and Pt(111), the Pt particles expose top facets in the (111) orientation.[45] The CO uptake measured by TPD on the annealed samples dropped almost to zero, that is a benchmark for the SMSI state via encapsulation. Moreover, the high resolution STM image (inset of Figure 5a) shows that the top facets exhibit the hexagonal lattice of protrusions with a ∼3 Å periodicity in turn forming a superstructure with a ∼25 Å periodicity. This structure is well-documented for a FeO(111) film on top of Pt(111), consisting of close-packed monolayers of iron and oxygen, that is, O−Fe−Pt(111).[46] Apparently, the driving force for the encapsulation is the high adhesion energy between Pt and iron oxide (ca. 4 J/m²) derived from the structural information provided by STM.

The Pt/Fe_3O_4(111) and FeO(111)/Pt(111) model catalysts were examined employing CO oxidation reaction at near-atmospheric pressures and relatively low temperatures.[47] Figure 5b shows kinetics of CO_2 production under O-rich conditions (10 mbar CO + 50 mbar O_2) over two Pt/Fe_3O_4-(111) samples possessing the same amount of Pt (∼2 ML). Prior to the reaction, one sample was annealed at 600 K and as such exposed a clean Pt surface, as judged by CO TPD,
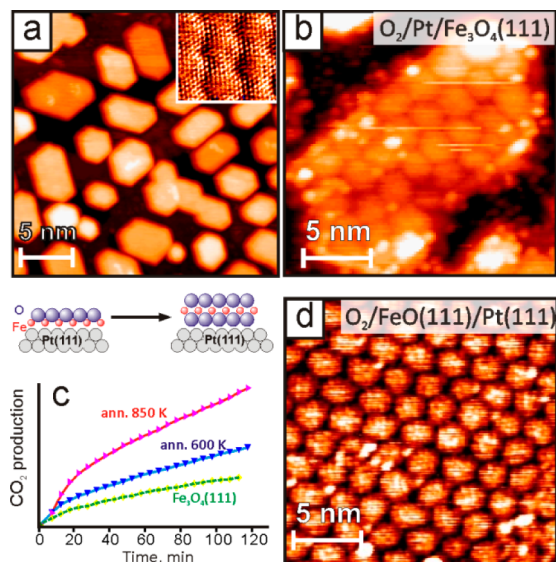
FIGURE 5. (a) STM image of Pt deposited onto a $Fe_3O_4(111)$ film and subsequently annealed in UHV at 850 K. High resolution image of the top facet is shown in the inset. (b) STM image of the encapsulated Pt particle exhibiting the same surface reconstruction (shown in the scheme) as a FeO(111)/Pt(111) film (d), both exposed to 20 mbar O_2 at 450 K. (c) CO_2 production over a clean $Fe_3O_4(111)$ film and two Pt/$Fe_3O_4(111)$ model catalysts, annealed in UHV to 600 and 850 K, respectively, prior to the reaction in 10 mbar CO + 50 mbar O_2 (He balance) at 450 K.

whereas another one was annealed at 850 K and hence encapsulated by the FeO layer. It is clear that the encapsulated Pt particles exhibit considerably higher reactivity than the clean Pt particles. This difference is even higher if one normalizes the reactivity to the particles surface area, which decreases at 850 K due to particle sintering. The same rate enhancement was observed also at the stoichiometric ratio (40 mbar CO + 20 mbar O_2). To rationalize such promotional effect of encapsulation we have to address the structure−reactivity relationships of well-ordered FeO(111) films on Pt(111).

As expected, the dense FeO(111) film on Pt(111) is essentially inert under conditions typically applied in UHV-based experiments. However, the same film shows considerable CO oxidation activity when the reaction is performed at mbar-range of pressures and relatively low temperatures (400−470 K). The experimental results in combination with DFT calculations[44] provided compelling evidence that the bilayer FeO(111) film transforms at elevated pressures into a trilayer O−Fe−O film. The proposed mechanism for this transformation starts by O_2 adsorption on an Fe atom pulled out of the pristine FeO film. The topmost O atoms in the FeO_{2-x} films formed are more weakly bound than those in the original FeO(111) bilayer and can readily react with

incoming CO to form CO_2, which then desorbs and leaves an oxygen vacancy behind. To end the catalytic cycle, the oxygen vacancies are replenished via reaction with O_2. Recent STM studies[48] provided strong evidence for this mechanism of Mars−van Krevelen type. Interestingly, NO transforms the FeO film into the trilayer film in the same way as O_2.[49] Comparison of the CO + O_2 and CO + NO reactions over the FeO(111)/Pt(111) surface suggest that the replenishment of oxygen vacancies is the rate-limiting step that proceeds much faster with O_2 than NO.

Apparently, the same scenario holds true for the FeO-encapsulated Pt particles. Indeed, Figure 5b,d shows STM images of large encapsulated Pt particles on $Fe_3O_4(111)$ and, for comparison, of a FeO(111)/Pt(111) film, both exposed to 20 mbar O_2 at 450 K, which exhibit very similar surface morphology. This similarity suggests basically the same reaction mechanism as observed on extended FeO/Pt(111) surfaces.

The above example demonstrates that ultrathin oxide films formed as modifiers on metal particles may have a promotional effect on reactivity, particularly in oxidation reactions at low temperatures, where pure metal catalysts may suffer from site-blocking effects and strong chemisorption of reactants. These results may aid in a deeper understanding of the reactivity of metal catalysts supported on reducible oxides, which exhibit "Strong Metal−Support Interaction".

Concluding Remarks

The investigation of model catalysts based on supported nanoparticles has proven successful for mimicking structural properties of real catalytic surfaces, holding a great potential to provide fundamental insight into heterogeneous catalysis. Via four case studies presented in this Account, we discussed how certain complex features, typically observed for technical catalytic materials, affect the growth mode (3D vs 2D) and catalytic performance of supported metallic nanoparticles. In the studies presented, we mainly focus on the effect of dopants and surface modifiers, which are often found to play a crucial role in catalytic performance, as well as on the dynamic changes of the active surface triggered by surface reactions and high-pressure conditions. In particular, doping of oxide materials opens promising routes to alter the morphology and electronic properties of supported metal particles and induce direct dissociation and reaction processes of molecules bound to the oxide surface. Furthermore, the small particle size and atomic flexibility of metal clusters can have a decisive influence on adsorption and

catalytic properties. For supported Pd nanoparticles, reduction of the particle size results in a strong reduction of the CO adsorption energy and, consequently, can strongly affect the equilibrium coverage of the surface species. The lateral flexibility of Pd nanoparticles was shown to be a highly important structural feature for hydrogenation of the olefinic double bond. Here, carbon adsorption at the laterally flexible low-coordinated surface sites, such as edges and corners, results in a local expansion of Pd lattice and formation of channels for barrier less diffusion of hydrogen into the volume of Pd nanoparticles. This vanishing activation barrier for subsurface H diffusion leads to a fast replenishment of subsurface H species, whose presence is necessary for hydrogenation of the C=C bond and sustained hydrogenation activity of Pd nanoparticles. These findings illustrate a very complex interplay between the inherent structural properties of metallic nanoparticles, such as atomic flexibility, and the effects of surface modifiers. Another case of surface modification, triggered by high pressure conditions, was observed for systems exhibiting a strong interaction with a reducible oxide support, that is, Pt/Fe_3O_4-(111). At technically relevant oxygen pressures, an active trilayer O−Fe−O film is formed on Pt surfaces, which was identified to be responsible for the high catalytic activity toward CO oxidation at low temperatures.

BIOGRAPHICAL INFORMATION

Swetlana Schauermann studied chemistry and received her Ph.D. in the group of H.-J. Freund investigating the catalytic activity of model supported nanoparticles by molecular beam techniques and vibrational spectroscopy. Between 2006 and 2007, she worked as a postdoctoral fellow with R. M. Lambert (Cambridge University) and C. T. Campbell (University of Washington) and later became a group leader in Fritz-Haber-Institut. Her current research is focused on thermodynamics of gas−surface interactions and on kinetics of complex surface reactions.

Niklas Nilius studied physics and received his Ph.D. in the group of H.-J. Freund investigating the optical properties of single metal particles by Photon-STM. Between 2002 and 2003, he worked as a

postdoctoral fellow with Wilson Ho on the properties of atomic chains artificially assembled on metal surfaces. His current research is focused on the adsorption characteristic of thin oxide films and on local optical properties of oxide surfaces.

Shamil Shaikhutdinov has received his Ph.D. (1986) in Physics from the Moscow Institute of Physics and Technology. Then he joined the group of K. Zamaraev at the Boreskov Institute of Catalysis (Novosibirsk) working on the application of surface science techniques to catalytic systems. From 1998 he worked as a postdoctoral fellow at the Fritz-Haber-Institute where he became a group leader in 2004. His research interest is focused on an understanding of structure−reactivity relationships in heterogeneous catalysis.

Hans-Joachim Freund studied physics and chemistry at the University of Cologne where he received his Ph.D. in 1978 and his habilitation in 1983. Between 1979 and 1981, he worked in the Physics Department at the University of Pennsylvania as a postdoctoral fellow. In 1983, he became Associate Professor at Erlangen University and in 1987 Professor at Bochum University. In 1995, he accepted a position as scientific member and director of the Department of Chemical Physics at the Fritz-Haber-Institut der Max-Planck-Gesellschaft in Berlin. He serves as Honorary Professor of five universities. He received several national and international awards, and he is a member of several academies, scientific societies, and advisory boards of scientific journals.

REFERENCES

1 Ertl, G.; Knözinger, H.; Weitkamp, J. *Handbook of Heterogeneous Catalysis*; VCH: Weinheim, 1997.

2 Henry, C. R. Surface studies of supported model catalysts. *Surf. Sci. Rep.* **1998**, *31*, 231–326.

3 Bäumer, M.; Freund, H.-J. Metal Deposits on Well-ordered Oxide Films. *Prog. Surf. Sci.* **1999**, *61*, 127–198.

4 Campbell, C. T.; Grant, A. W.; Starr, D. E.; Parker, S. C.; Bondzie, V. A. Model oxide-supported metal catalysts: energetics, particle thicknesses, chemisorption and catalytic properties. *Top. Catal.* **2001**, *14*, 43–51.

5 Risse, T.; Shaikhutdinov, S.; Nilius, N.; Sterrer, M.; Freund, H.-J. Gold Supported on Thin Oxide Films: From Single Atoms to Nanoparticles. *Acc. Chem. Res.* **2008**, *41*, 949–956.

6 Hashmi, A. S. K.; Hutchings, G. J. Gold Catalysis. *Angew. Chem., Int. Ed.* **2006**, *45*, 7896–7936.

7 Herzing, A. A.; Kiely, C. J.; Carley, A. F.; Landon, P.; Hutchings, G. J. Identification of Active Gold Nanoclusters on Iron Oxide Supports for CO Oxidation. *Science* **2008**, *321*, 1331–1335.

8 Valden, M.; Lai, X.; Goodman, D. W. Onset of Catalytic Activity of Gold Clusters on Titania with the Appearance of Nonmetallic Properties. *Science* **1998**, *281*, 1647–1650.

9 Chen, M. S.; Goodman, D. W. The Structure of Catalytically Active Au on Titania. *Science* **2004**, *306*, 252–255.

10 Pacchioni, G.; Giordano, L.; Baistrocchi, M. Charging of Metal Atoms on Ultrathin MgO/Mo(100) Films. *Phys. Rev. Lett.* **2005**, *94*, 226104–1−4.

11 Nilius, N.; Ganduglia-Pirovano, M. V.; Brázdová, V.; Kulawik, M.; Sauer, J.; Freund, H. J. Counting Electrons Transferred through a Thin Alumina Film into Au Chains. *Phys. Rev. Lett.* **2008**, *100*, 096802–1−4.

12 Sterrer, M.; Risse, T.; Heyde, M.; Rust, H.-P.; Freund, H.-J. Crossover from Three-Dimensional to Two-Dimensional Geometries of Au Nanostructures on Thin MgO(001) Films: A Confirmation of Theoretical Predictions. *Phys. Rev. Lett.* **2007**, *98*, 206103–1−4.

13 Shao, X.; Nilius, N.; Freund, H.-J. Crossover from two- to three-dimensional gold particle shapes on CaO films of different thicknesses. *Phys. Rev. B* **2012**, *85*, 115444–1−8.

14 Li, B.; Metiu, H. DFT Studies of Oxygen Vacancies on Undoped and Doped La_2O_3 Surfaces. *J. Phys. Chem. C* **2010**, *114*, 12234–12244.

15 Hu, Z.; Li, B.; Sun, X.; Metiu, H. Chemistry of Doped Oxides: The Activation of Surface Oxygen and the Chemical Compensation Effect. *J. Phys. Chem. C* **2011**, *115*, 3065–3074.

16 Shao, X.; Prada, S.; Giordano, L.; Pacchioni, G.; Nilius, N.; Freund, H.-J. Tailoring the Shape of Metal Ad-Particles by Doping the Oxide Support. *Angew. Chem., Int. Ed.* **2011**, *50*, 11525–11527.

17 Stavale, F.; Shao, X.; Nilius, N.; Freund, H.-J.; Prada, S.; Giordano, L.; Pacchioni, G. Donor Characteristics of Transition-Metal-Doped Oxides: Cr-Doped MgO versus Mo-Doped CaO. *J. Am. Chem. Soc.* **2012**, *134*, 11380–11383.

18 Benia, H. M.; Myrach, P.; Gonchar, A.; Risse, T.; Nilius, M.; Freund, H. J. Electron trapping in misfit dislocations of MgO thin films. *Phys. Rev. B* **2010**, *81*, 241415–1—4.

19 Shao, X.; Nilius, N.; Freund, H.-J. Li/Mo Codoping of CaO Films: A Means to Tailor the Equilibrium Shape of Au Deposits. *J. Am. Chem. Soc.* **2012**, *134*, 2532–2534.

20 Fischer-Wolfarth, J.-H.; Farmer, J. A.; Flores-Camacho, J. M.; Genest, A.; Yudanov, I. V.; Rösch, N.; Campbell, C. T.; Schauermann, S.; Freund, H.-J. Particle-size dependent heats of adsorption of CO on supported Pd nanoparticles as measured with a single-crystal microcalorimeter. *Phys. Rev. B* **2010**, *81*, 241416-1–241416-4.

21 Stará, I.; Matolín, V. The influence of particle size on CO adsorption on Pd/alumina model catalysts. *Surf. Sci.* **1994**, *313*, 99–106.

22 Borronibird, C. E.; King, D. A. An Ultrahigh-Vacuum Single-Crystal Adsorption Micro-calorimeter. *Rev. Sci. Instrum.* **1991**, *62*, 2177–2185.

23 Stuckless, J. T.; Frei, N. A.; Campbell, C. T. A novel single-crystal adsorption calorimeter and additions for determining metal adsorption and adhesion energies. *Rev. Sci. Instrum.* **1998**, *69*, 2427–2438.

24 Yudanov, I. V.; Sahnoun, R.; Neyman, K. M.; Rösch, N.; Hoffmann, J.; Schauermann, S.; Johanek, V.; Unterhalt, H.; Rupprechter, G.; Libuda, J.; Freund, H. J. CO adsorption on Pd nanoparticles: Density functional and vibrational spectroscopy studies. *J. Phys. Chem. B* **2003**, *107*, 255–264.

25 Campbell, C. T.; Ertl, G.; Kuipers, H.; Segner, J. A molecular beam investigation of the interactions of CO with a Pt(111) surface. *Surf. Sci.* **1981**, *107*, 207–219.

26 Nepijko, S. A.; Klimenkov, M.; Adelt, M.; Kuhlenbeck, H.; Schlögl, R.; Freund, H.-J. Structural investigation of palladium clusters on g-Al$_2$O$_3$(111)/NiAl(110) with transmission electron microscopy. *Langmuir* **1999**, *15*, 5309–5313.

27 Krüger, S.; Vent, S.; Nörtemann, F.; Staufer, M.; Rösch, N. The average bond length in Pd clusters Pd$_n$, n = 4—309: A density-functional case study on the scaling of cluster properties. *J. Chem. Phys.* **2001**, *115*, 2082–2087.

28 Yudanov, I. V.; Metzner, M.; Genest, A.; Rösch, N. Size-Dependence of Adsorption Properties of Metal Nanoparticles: A Density Functional Study on Palladium Nanoclusters. *J. Phys. Chem. C* **2008**, *112*, 20269–20275.

29 Shustorovich, E.; Sellers, H. The UBI-QEP method: A practical theoretical approach to understanding chemistry on transition metal surfaces. *Surf. Sci. Rep.* **1998**, *31*, 1–119.

30 Yudanov, I. V.; Genest, A.; Schauermann, S.; Freund, H.-J.; Rösch, N. Size Dependence of the Adsorption Energy of CO on Metal Nanoparticles: A DFT Search for the Minimum Value. *Nano Lett.* **2012**, *12*, 2134–2139.

31 to be published.

32 Bond, G. C. *Metal-Catalysed Reactions of Hydrocarbons*; Springer: New York, 2005.

33 Wilde, M.; Fukutani, K.; Ludwig, W.; Brandt, B.; Fischer, J.-H.; Schauermann, S.; Freund, H. J. Influence of Carbon Deposition on the Hydrogen Distribution in Pd Nanoparticles and Their Reactivity in Olefin Hydrogenation. *Angew. Chem., Int. Ed.* **2008**, *47*, 9289–9293.

34 Ludwig, W.; Savara, A.; Schauermann, S.; Freund, H.-J. Role of Low-Coordinated Surface Sites in Olefin Hydrogenation: A Molecular Beam Study on Pd Nanoparticles and Pd(111). *ChemPhysChem* **2010**, *11*, 2319–2322.

35 Ludwig, W.; Savara, A.; Dostert, K.-H.; Schauermann, S. Olefin hydrogenation on Pd model supported catalysts: New mechanistic insights. *J. Catal.* **2011**, *284*, 148–156.

36 Wilde, M.; Fukutani, K.; Naschitzki, M.; Freund, H. J. Hydrogen absorption in oxide-supported palladium nanocrystals. *Phys. Rev. B* **2008**, *77*, 113412–1—6.

37 Viñes, F.; Loschen, C.; Illas, F.; Neyman, K. M. Edge sites as a gate for subsurface carbon in palladium nanoparticles. *J. Catal.* **2009**, *266*, 59–63.

38 Doyle, A. M.; Shaikhutdinov, S. K.; Jackson, S. D.; Freund, H.-J. Hydrogenation on Metal Surfaces: Why are Nanoparticles More Active than Single Crystals? *Angew. Chem., Int. Ed.* **2003**, *42*, 5240–5243.

39 Neyman, K. M.; Schauermann, S. Hydrogen Diffusion into Palladium Nanoparticles: Pivotal Promotion by Carbon13. *Angew. Chem., Int. Ed.* **2010**, *49*, 4743–4746.

40 Ludwig, W.; Savara, A.; Madix, R. J.; Schauermann, S.; Freund, H.-J. Subsurface Hydrogen Diffusion into Pd Nanoparticles: Role of Low-Coordinated Surface Sites and Facilitation by Carbon. *J. Phys. Chem. C* **2012**, *116*, 3539–3544.

41 Tauster, S. J. Strong metal-support interactions. *Acc. Chem. Res.* **1987**, *20*, 389–394.

42 Dulub, O.; Hebenstreit, W.; Diebold, U. Imaging Cluster Surfaces with Atomic Resolution: The Strong Metal-Support Interaction State of Pt Supported on TiO$_2$(110). *Phys. Rev. Lett.* **2000**, *84*, 3646–3649.

43 Bowker, M.; Stone, P.; Morrall, P.; Smith, R.; Bennett, R.; Perkins, N.; Kvon, R.; Pang, C.; Fourre, E.; Hall, M. Model catalyst studies of the strong metal—support interaction: Surface structure identified by STM on Pd nanoparticles on TiO2(110). *J. Catal.* **2005**, *234*, 172–181.

44 Sun, Y.-N.; Giordano, L.; Goniakowski, J.; Lewandowski, M.; Qin, Z.-H.; Noguera, C.; Shaikhutdinov, S.; Pacchioni, G.; Freund, H.-J. The Interplay between Structure and CO Oxidation Catalysis on Metal-Supported Ultrathin Oxide Films. *Angew. Chem., Int. Ed.* **2010**, *49*, 4418–4421.

45 Qin, Z. H.; Lewandowski, M.; Sun, Y. N.; Shaikhutdinov, S.; Freund, H. J. Morphology and CO adsorption on platinum supported on thin Fe$_3$O$_4$(111) films. *J. Phys.: Condens. Matter* **2009**, *21*, 134019-1–134019-6.

46 Ritter, M.; Ranke, W.; Weiss, W. Growth and structure of ultrathin FeO films on Pt(111) studied by STM and LEED. *Phys. Rev. B* **1998**, *57*, 7240–7251.

47 Sun, Y. N.; Qin, Z. H.; Lewandowski, M.; Carrasco, E.; Sterrer, M.; Shaikhutdinov, S.; Freund, H. J. Monolayer iron oxide film on platinum promotes low temperature CO oxidation. *J. Catal.* **2009**, *266*, 359–368.

48 Lewandowski, M.; Groot, I. M. N.; Shaikhutdinov, S.; Freund, H. J. Scanning tunneling microscopy evidence for the Mars-van Krevelen type mechanism of low temperature CO oxidation on an FeO(111) film on Pt(111). *Catal. Today* **2012**, *181*, 52–55.

49 Lei, Y.; Lewandowski, M.; Sun, Y.-N.; Fujimori, Y.; Martynova, Y.; Groot, I. M. N.; Meyer, R. J.; Giordano, L.; Pacchioni, G.; Goniakowski, J.; Noguera, C.; Shaikhutdinov, S.; Freund, H.-J. CO+NO versus CO+O$_2$ Reaction on Monolayer FeO(111) Films on Pt(111). *ChemCatChem* **2011**, *3*, 671–674.